AD-A095 626 STANFORD UNIV CA F/G 12/1
SOME BUBBLE AND CONTACT PROBLEMS,(U)
NOV 79 J B KELLER DAAG29-79-C-0222
UNCLASSIFIED ARO-16997.7-M NL

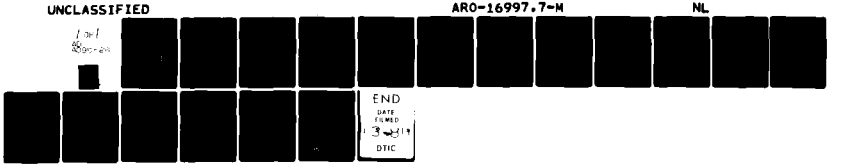

END
DATE FILMED
3-80
DTIC

(18) ARO

UNCLASSIFIED

SECURITY CLASSIFICATION OF THIS PAGE (When Data Entered)

(2)

REPORT DOCUMENTATION PAGE	READ INSTRUCTIONS BEFORE COMPLETING FORM
(19) 1. REPORT NUMBER: 16997.7-M	2. GOVT ACCESSION NO: AD-A095 626
	3. RECIPIENT'S CATALOG NUMBER: N/A
(6) 4. TITLE (and Subtitle): Some Bubble and Contact Problems	5. TYPE OF REPORT & PERIOD COVERED: REPRINT
(10)	6. PERFORMING ORG. REPORT NUMBER: N/A
7. AUTHOR(s): Joseph B. Keller (11) 21 Nov 71 (15)	8. CONTRACT OR GRANT NUMBER(s): DAAG29-79-C-0222
9. PERFORMING ORGANIZATION NAME AND ADDRESS: Stanford University, Stanford, CA 94305 (12) 11	10. PROGRAM ELEMENT, PROJECT, TASK AREA & WORK UNIT NUMBERS: N/A
11. CONTROLLING OFFICE NAME AND ADDRESS: US Army Research Office, PO Box 12211, Research Triangle Park, NC 27709	12. REPORT DATE: Oct 80
	13. NUMBER OF PAGES: 17
14. MONITORING AGENCY NAME & ADDRESS (if different from Controlling Office)	15. SECURITY CLASS. (of this report): Unclassified
	15a. DECLASSIFICATION/DOWNGRADING SCHEDULE

16. DISTRIBUTION STATEMENT (of this Report)

Submitted for announcement only

17. DISTRIBUTION STATEMENT (of the abstract entered in Block 20, if different from Report)

DTIC ELECTE FEB 27 1981 S B

18. SUPPLEMENTARY NOTES

19. KEY WORDS (Continue on reverse side if necessary and identify by block number)

20. ABSTRACT (Continue on reverse side if necessary and identify by block number)

AD A095626

DTIC FILE COPY

DD FORM 1 JAN 73 1473 EDITION OF 1 NOV 65 IS OBSOLETE

UNCLASSIFIED

SECURITY CLASSIFICATION OF THIS PAGE (When Data Entered)

ARO 16997.7-M

SIAM REVIEW
Vol. 22, No. 4, October 1980

SOME BUBBLE AND CONTACT PROBLEMS*

JOSEPH B. KELLER†

Abstract. A number of problems involving bubbles in a fluid, or contact of surfaces, or both are considered. In each case the size and/or the shape of the bubble, or the location of the points of contact, are unknown in advance and must be found. When the problems are formulated mathematically, boundary conditions must be satisfied at the bubble surface and at the contact points, which are thus "free" boundaries. The problems are: postbuckling behavior of an elastic tube, contact problems involving a buckled elastica, steep capillary waves with trapped bubbles, deformation of a bubble in a uniform flow, distortion of a bubble in a straining flow, free oscillation of an underwater explosion bubble, and forced oscillation of a bubble in a sound field.

1. Introduction. Physical problems involving bubbles or drops in a fluid generally require the determination of the size and/or the shape of the bubble or drop surface. Problems involving the contact of elastic or fluid surfaces usually require the location of the points of contact. In both cases, boundary conditions must be satisfied at the unknown bubble or drop surface or contact point. Thus these surfaces or points are "free" boundaries, which must be found as part of the solution of the problem. In the case of bubbles in contact with themselves or with other surfaces, there are contact points on the bubble surface. These points are thus free boundaries of free boundaries, which might be called "free free boundaries".[1]

With the help of a number of coworkers, I have analyzed various free boundary problems involving bubbles and/or contact of surfaces. I shall describe some of them in this report, emphasizing the reasons for considering them, the principles involved in their formulation, and the nature of the results. In all cases, some analytical results and some numerical results were obtained. I shall present some of the numerical results and some figures based on them, indicating what the numerical methods were when that seems appropriate. I shall just mention the analytical results, referring for their detailed presentation to the relevant published articles.

The goal of this report is to show that certain problems involving contact of surfaces can be formulated and analyzed in a relatively simple way. In some cases, the maintenance of contact is required to prevent the unphysical phenomenon of a surface crossing over itself. When the surface is a fluid-fluid interface, the resulting contact may lead to the occurrence of bubbles or drops. When the bubbles or drops are deformed, parts of their surfaces may again come into contact with one another and form new bubbles or drops. Since phenomena involving the contact of surfaces are of widespread occurrence, it is to be hoped that the results reported here will stimulate further investigations of them.

2. Postbuckling behavior of an elastic tube. While investigating blood flow in arteries and veins, my colleague S. I. Rubinow and I realized that the pressure of the blood in a vein could fall below the ambient pressure outside the vein. As a consequence, the wall of the vein could buckle, thus changing the vein cross section from circular to some other shape, and thereby increasing the vein's resistance to blood

* Received by the editors November 21, 1979

† Departments of Mathematics and Mechanical Engineering, Stanford University, Stanford, California 94305. This report is based upon a lecture presented by the author upon receiving the Theodore von Karman Prize at the Fall Meeting of the Society for Industrial and Applied Mathematics in Denver, Colorado on November 13, 1979. This work was supported by the Office of Naval Research, the National Science Foundation, the Air Force Office of Scientific Research and the Army Research Office.

[1] Whitham [1, p. 289] has called discontinuity lines on shock surfaces "shock shocks".

flow. Therefore, with J. E. Flaherty [2], we studied the buckling and postbuckling behavior of an elastic tube.

We assumed that, for any given pressure difference p, the equilibrium configuration of the tube would be a cylinder, and we denoted by C its cross sectional curve. Then the equations of elastostatics governing the tube are the same as those of an elastic ring C compressed by a force p per unit length. This problem had been studied by I. Tadjbakhsh and F. Odeh [3]. They assumed that the ring is inextensible and is governed by the Euler–Bernoulli beam theory, with the bending moment proportional to $k(s) - 1$. Here $k(s)$ is the curvature of C at arclength s along it, and 1 is the curvature when C is a circle. In dimensionless variables these assumptions lead to the equation

$$k'' + \tfrac{1}{2}k^3 - ck - p = 0, \qquad 0 \leqq s \leqq 2\pi. \tag{2.1}$$

Here c is a constant to be determined. In addition, k must be periodic with period 2π, and the integral of k over a period must be 2π. This latter condition follows from the fact that $k(s) = \theta'(s)$, where $\theta(s)$ is the angle between the tangent to C and some fixed direction.

For every value of $p > 0$, this problem has a solution $k(s) \equiv 1$ and $c = \frac{1}{2} - p$, corresponding to C being a circle. As Tadjbakhsh and Odeh [3] showed, this unbuckled solution is the only solution for $p \leqq 3$, while for $p > 3$ there are other solutions. Each other solution is periodic with period $2\pi/n$ for some integer $n \geqq 2$ and, for a suitable origin of s, it is odd in s. Thus each such solution satisfies the conditions

$$k(0) = 0, \quad k'(\pi/n) = 0, \quad \int_0^{\pi/n} k(s)\,ds = \pi/n. \tag{2.2}$$

Furthermore, it exists only for $p > p_{n*}$, where p_{n*} is called the nth buckling load. They computed the solutions numerically for the first few values of n for a range of $p > p_{n*}$. For the nth solution, when p reached a second critical value p_{nn}, $n > 2$, n pairs of points came into contact with one another, while for $n = 2$, one pair of opposite points came into contact. For $p > p_{nn}$, the ring crossed over itself.

Crossing over may be possible for opposite parts of a ring, if one part comes out of the plane containing the rest of the ring. However it is not possible for a tube. Therefore we reexamined the problem for the nth solution with $p > p_{nn}$, to find a solution which does not cross over itself. We required that for $p > p_{nn}$ one pair of points in each period be in contact with one another. For $n = 2$, these points are the endpoints of the period, so there is only one pair in contact, and they are at $s = \pm\pi/2$. For $n > 2$ the locations $\pm s_1$ of the contact points must be determined.

In the case $n > 2$ we found that the second condition in (2.2) had to be changed so that (2.2) became

$$k(0) = 0, \quad k(\pi/2) = 2, \quad \int_0^{\pi/2} k(s)\,ds = \pi/2 \quad \text{for } p \geqq p_{n2}. \tag{2.3}$$

We solved (2.1) and (2.2) numerically to obtain $k(s)$ and c for various values of p from $p = p_{n*} + 3$ up to $p = p_{n2} = 5.247$. Then we solved (2.1) and (2.3) for p from $p = p_{n2} = 5.247$ up to $p = p_{nn} = 10.34$ when the curvature $k(\pi/2)$ at the contact point became zero. For $p > p_{nn}$ we assumed that the solution has an interval of contact extending from some value $s = s_1 > 0$ up to $s = \pi/2$. Then we showed that s_1 and the shape of the remaining part of the solution could be obtained by a similarity transformation from the result for $p = p_{nn}$. The results are shown in Fig. 1, and corresponding results for $n = 4$ are shown in Fig. 2.

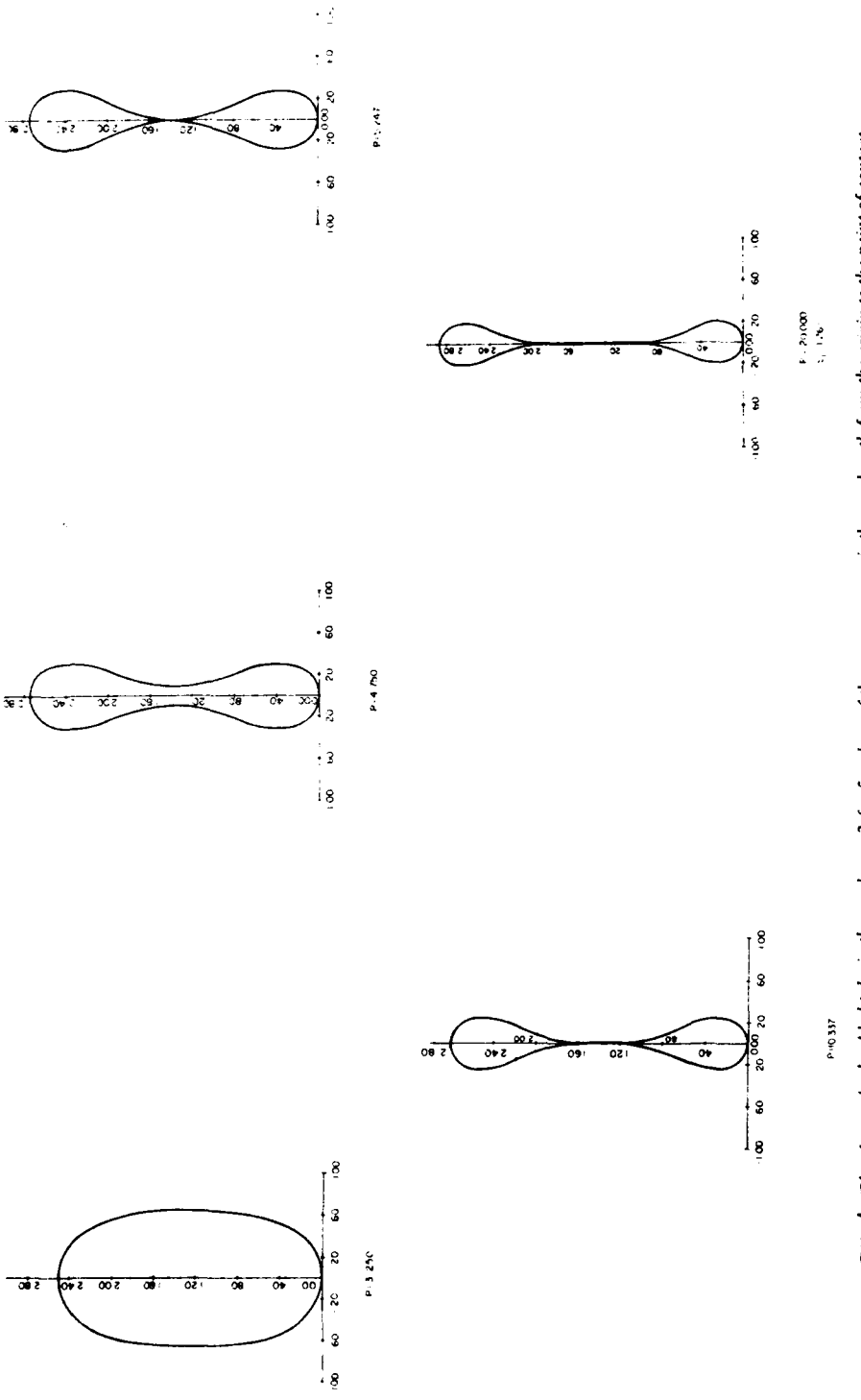

FIG. 1. *The shape of a buckled tube in the mode $n = 2$ for 5 values of the pressure p. s_1 is the arc length from the origin to the point of contact.*

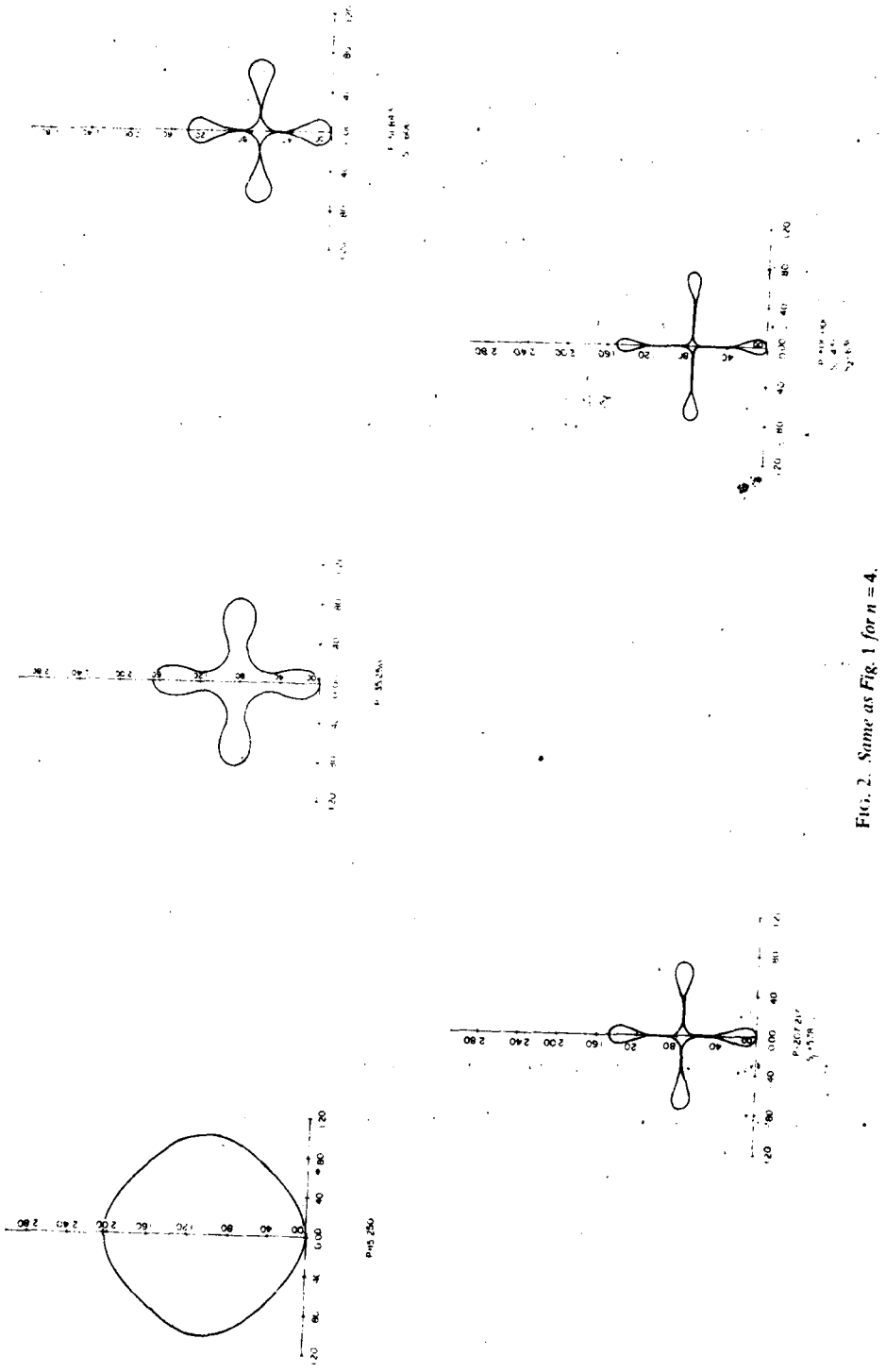

FIG. 2. *Same as Fig. 1 for n = 4.*

Once we had the shape of the tube's cross section for $n = 2$ and each value of p, we solved the equation $\Delta u = -1$ within the cross section with $u = 0$ on the boundary for each p. This yielded the velocity of the flow of a viscous fluid along the tube. The results showed that the conductivity of the tube, i.e., the flux of fluid for unit pressure gradient along the tube, decreased drastically when the tube began to buckle. These results have been confirmed quantitatively by the experiments of H. Zeller and R. Wirtz [4]. They measured the flow through a rubber tube buckled by a pressure difference p, and their results agreed fairly well with our calculations, as is shown in Fig. 3. Their corresponding results for a tube of polyvinylchloride (PVC), also shown in Fig. 3, do not agree so well, although they would do so if the Young's modulus E used in scaling the horizontal axis were replaced by $E/2$. The cross sections of buckled Penrose tubing in various stages of collapse during flow look like the cross sections in Fig. 2 (see [5], [6]), as do the cross sections of the vena cava in normal breathing [7].

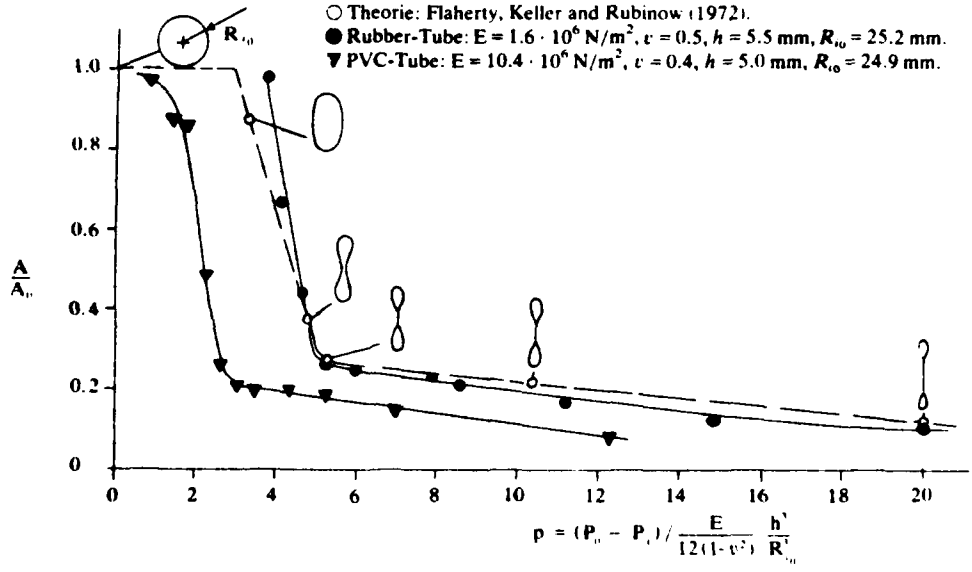

FIG. 3. *The normalized flow through a tube as a function of the pressure difference between the outside and the inside. The open circles and the dashed curve are based on the theory described in § 2. The black circles are experimental values for a rubber tube measured by H. Zeller and R. Wirtz* [4]. *The black triangles are their measured values for a tube made of polyvinylchloride (PVC). They would have agreed better with the theory if a smaller value had been used for Young's modulus E of PVC.*

3. Contact problems for a buckled elastica. In 1744, Euler formulated and solved the problem of the buckling of a thin elastic rod or column, which he called an "elastica", subject to a compressive load P at its ends. He found that a rod clamped at its ends remained straight or unbuckled for $0 \leqq P \leqq P_{b1} = 4\pi^2$, where P_{b1} is the dimensionless first buckling load. For $P > P_{b1}$ the rod could buckle, and as P increased it deformed more and more until a pair of points came into contact at some value P_{c1}. For $P > P_{c1}$ the elastica crossed over itself. If we consider the elastica to lie in a plane, or to be a cross section of a cylindrical elastic sheet, it cannot cross itself. Therefore J. E. Flaherty and I sought a solution for $P > P_{c1}$ which did not do so [8].

In dimensionless variables, we let $\theta(s)$ be the angle between the x-axis and the tangent to the elastica at arclength position s, with s ranging from 0 to 1. Then the

equation of equilibrium, according to the Euler–Bernoulli beam theory, is

$$\theta_{ss} + P \sin\theta = 0, \qquad 0 \leqq s \leqq 1. \tag{3.1}$$

The condition that the ends are clamped along the x-axis yields

$$\theta(0) = 0, \quad \theta(1) = 0, \quad \int_0^1 \sin\theta(s)\, ds = 0. \tag{3.2}$$

We solved (3.1) and (3.2) numerically for various values of P from $P_{b1} = 4\pi^2$ to $P_{c1} = 72.187$, at which contact first occurs. (See Fig. 4.)

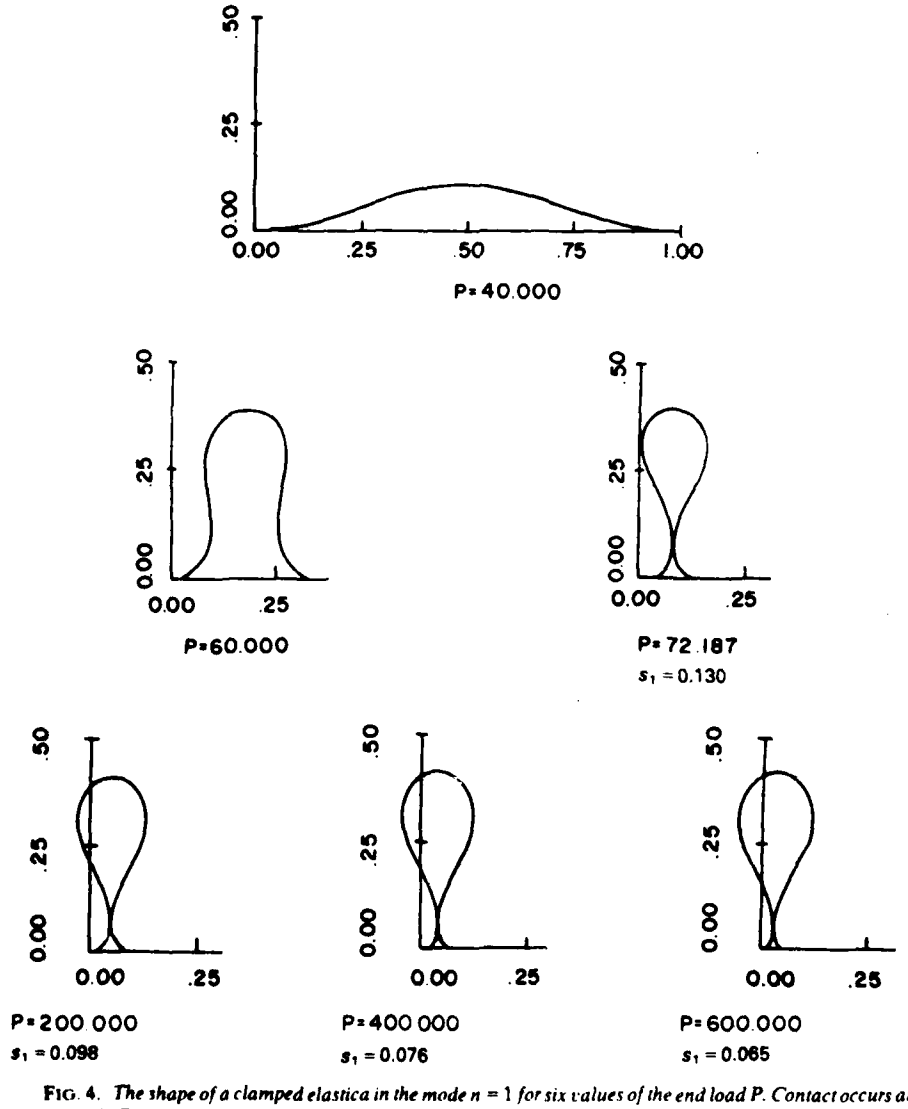

FIG. 4. *The shape of a clamped elastica in the mode $n = 1$ for six values of the end load P. Contact occurs at $P_c = 72.187$. For $P > P_c$ the similarity solution was used to compute the shape of the loop between the points of contact.*

For $P > P_{c1}$, we require contact to occur between the two points s_1 and $1 - s_1$, with s_1 to be found in the range $0 < s_1 < \frac{1}{2}$. Then (3.1) holds only in the intervals $0 < s < s_1$ and $1 - s_1 < s < 1$, while between these intervals it is replaced by

$$\theta_{ss} + (P - R)\sin\theta = 0, \qquad s_1 < s < 1 - s_1. \tag{3.3}$$

Here R is the contact force, which is to be found. We seek a solution in which $\theta(s)$ is antisymmetric about $s = \frac{1}{2}$, so it suffices to solve (3.1) for $0 < s < s_1$ and (3.3) for $s_1 < s < \frac{1}{2}$. In addition, we have the six conditions

$$\theta(0) = 0, \quad \theta(s_1) = \pi/2, \quad \theta(\tfrac{1}{2}) = 0, \quad \int_{s_1}^{1/2} \cos\theta(s)\, ds = 0, \quad \theta \text{ and } \theta_s \text{ continuous at } s_1. \tag{3.4}$$

These six conditions suffice to determine s_1, R and the two integration constants in each interval.

We found that the solution of (3.3), which describes the closed loop, could be determined for any $P > P_{c1}$ from the solution at P_{c1} by a similarity transformation. Therefore for $P > P_{c1}$ we only had to solve (3.1) numerically, together with the appropriate conditions from (3.4).

The results for three such values are shown in Fig. 4. We also found that, for P large, s_1 is given by

$$s_1 \sim 1.854P^{-1/2} - 6.055P^{-1}, \qquad P \gg 1. \tag{3.5}$$

Thus the contact points approach the endpoints as P tends to infinity.

These results can be confirmed qualitatively, with a strip of flexible plastic, by holding one end in each hand and bringing the ends toward one another.

4. Capillary waves with trapped bubbles. Sufficiently short waves on the surface of a liquid are governed mainly by surface tension. For many years such capillary waves were studied on the assumption that the amplitude a was much less than the wavelength λ, so that the steepness $s = a/\lambda$ was small. Then it was possible to linearize the governing equations. In 1957, D. G. Crapper [9] sought to express the wave motion as a power series in s. From the regularity of the first few coefficients he guessed the general term, verified it, and then was able to sum the series in closed form. His result yielded waves ranging from sinusoidal waves for s small up to a steepest one at $s = .73$, when adjacent waves touched one another at one point. For $s > .73$, his result was unphysical since adjacent waves overlapped one another.

In view of the studies reported in the two preceding sections, I believed that it should be possible to obtain steeper waves by enforcing contact of adjacent waves and preventing overlap. Therefore J.-M. Vanden-Broeck and I [10] did just that. Following Crapper, we considered steady two-dimensional periodic capillary waves on the surface of an inviscid incompressible fluid of infinite depth. We considered the complex position $x + iy$ as a function of the complex potential $\varphi + i\psi$ in the halfplane $\psi \leqq 0$. The streamline $\psi = 0$ corresponded to the free surface. At it, the pressure in the fluid had to exceed the pressure in the air above the surface by the surface tension times the curvature of the surface. In dimensionless variables this led to the equation

$$(x_\varphi^2 + y_\varphi^2)^{-1} - 1 - T(x_\varphi y_{\varphi\varphi} - y_\varphi x_{\varphi\varphi})(x_\varphi^2 + y_\varphi^2)^{-3/2} = 0 \quad \text{on } \psi = 0. \tag{4.1}$$

Here T is a dimensionless constant proportional to the surface tension. The specification of the fluid velocity at $y = -\infty$ is that $(x_\varphi, y_\varphi) \to (1, 0)$ as $\psi \to -\infty$.

To complete the formulation of the problem, we employed the assumed periodicity in φ of the solution and the Hilbert transform to obtain

$$y_\varphi(\varphi, 0) = \int_0^{\frac{1}{2}} [x_\varphi(\varphi', 0) - 1][\cot \pi(\varphi' - \varphi) - \cos \pi(\varphi' - \varphi)]\, d\varphi'. \tag{4.2}$$

In terms of y_φ, the steepness s is given by

$$s = -\int_0^{\frac{1}{2}} y_\varphi(\varphi, 0)\, d\varphi. \tag{4.3}$$

Equations (4.1)–(4.3) constitute a problem for the determination of the periodic functions $x_\varphi(\varphi, 0)$, $y_\varphi(\varphi, 0)$ and T for a given value of s.

When s is large enough, we modify the preceding formulation by requiring contact to occur at the point $\varphi = \alpha$, $\psi = 0$ on the free surface, with α to be found in the interval $0 < \alpha < \frac{1}{2}$. Then at the contact point we require

$$x_\varphi(\alpha, 0) = 0, \qquad x(\alpha, 0) = \int_0^\alpha x_\varphi(\varphi, 0)\, d\varphi = \tfrac{1}{2}. \tag{4.4}$$

Since contact of adjacent waves results in a trapped bubble of air, we permit the pressure in the bubble to exceed the pressure in the air above the surface by the dimensionless amount P. Then we must replace the right side of (4.1) by P in the range $\alpha < \varphi \leqq \frac{1}{2}$.

We solved the problem without contact by introducing $N + 1$ equally spaced mesh points φ_i in the interval $0 \leqq \varphi \leqq 1$, the values $x_i' = x_\varphi(\varphi_i, 0)$, and the values y_i' of $y_\varphi(\varphi, 0)$ midway between adjacent mesh points. By using the trapezoidal rule in (4.2) we expressed the y_i' in terms of the x_i'. Then we used centered four-point interpolation and difference formulas to evaluate the derivatives in (4.1). In this way we converted (4.1) into a set of $N + 1$ nonlinear algebraic equations for the x_i', and (4.3) into an $(N + 2)$nd equation. We solved these equations by Newton's method for T and the $N + 1$ quantities x_i' using $N = 40$ and $N = 60$. The two sets of results agreed to four decimals with each other and with Crapper's solution.

To find solutions with contact, we introduced the two extra unknowns α and P, and the two extra equations (4.4). We also forced α to be a mesh point by separately subdividing the intervals $0 \leqq \varphi \leqq \alpha$ and $\alpha \leqq \varphi \leqq \frac{1}{2}$. Then we solved the resulting equations for α, P, T and the x_i' by Newton's method using 60 mesh points. For each value of s we used, as the initial approximation to the solution, the solution for a slightly smaller value of s, starting with Crapper's solution at $s = 0.730$.

We were able to find solutions with $s > 0.730$, and we computed them up to $s = 1.5$. It seems clear that we could compute them for any larger value of s by increasing the number of mesh points. Typical solutions are shown in Fig. 5. We also found solutions with $s < 0.730$, in the interval $0.663 < s < 0.730$, so that two solutions exist in this range—Crapper's and this new one. As s decreases to 0.663, the curvature of the surface at the contact point decreases to zero, which is why this family ends there. On the other hand, as $s \to \infty$, each bubble becomes infinitely long and narrow, with its width proportional to $e^{-2\pi s}$. Simultaneously the surface above them tends to a series of semicircles tangent to one another.

5. Deformation of a bubble in a uniform flow. Surface tension forces a bubble in a liquid at rest to become spherical in three dimensions and circular in two dimensions. But pressure forces due to a fluid flowing around a bubble can deform it to another shape. We have seen an example of this in the previous section, where the bubbles were

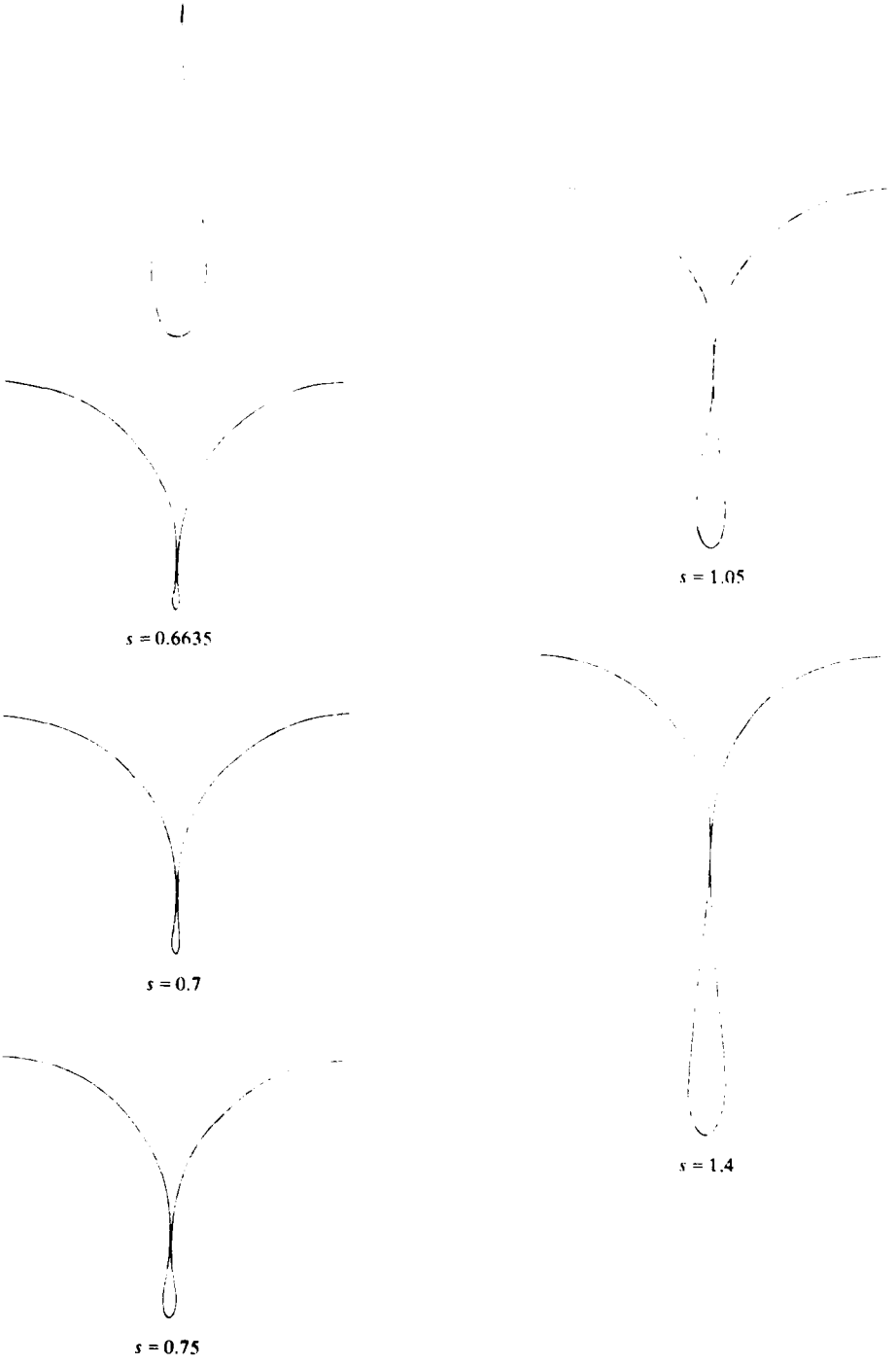

FIG. 5. *Computed profiles of the free surface and bubble for five values of s. The upper curve for the case* $s = 0.6635$ *shows the bubble on a scale expanded by a factor of* 10.

long and tapered at their upper ends. But in that case each bubble was affected by the presence of the upper surface and the other bubbles. It is more important to know how an isolated bubble is deformed, since bubbles often occur in isolation. Therefore J.-M. Vanden-Broeck and I [11] investigated this deformation.

We considered a two-dimensional bubble in a steady potential flow of an inviscid incompressible fluid. The flow was assumed to be uniform at infinity and the pressure within the bubble was assumed to be constant. On the unknown bubble boundary, the fluid velocity was required to be directed tangentially and the bubble pressure was required to exceed the fluid pressure by the surface tension multiplied by the curvature of the boundary. Upon introducing dimensionless variables, we found that the coefficient of surface tension σ could be eliminated by using $2\sigma/\rho U^2$ as the unit of length, where ρ is the density of the fluid and U is the velocity at infinity. Then the problem contained a single dimensionless parameter γ, defined by

$$\gamma = 2(p_b - p_s)/\rho U^2. \tag{5.1}$$

Here p_b is the pressure in the bubble and p_s is the stagnation pressure, which equals the pressure at infinity minus $\rho U^2/2$.

Before solving the problem, we required that the flow and the bubble be symmetric about the x-axis, which we took parallel to the velocity at infinity. Then it sufficed to consider the flow outside the bubble in the halfplane $y \geqq 0$. This flow region corresponded to the halfplane $\psi \geqq 0$ of the complex potential plane, and the bubble surface corresponded to the segment $-b < \tilde{\varphi} < b$ of the axis $\psi = 0$, with b unknown. It was convenient to set $\tilde{\varphi} = b\varphi$ so that the bubble surface corresponded to the segment $-1 < \varphi < 1$, $\psi = 0$. Then we sought $x - iy$ as an analytic function of $b\varphi + i\psi$ in this halfplane. The velocity at infinity was $(x_\varphi, y_\varphi) = (b, 0)$.

By applying Cauchy's theorem to $x + iy - b$ and, taking the real part, we obtained the Hilbert transform relation

$$x_\varphi(\varphi, 0) = b + \frac{1}{\pi}\int_{-1}^{1} \frac{y_\varphi(\varphi', 0)}{\varphi' - \varphi}\, d\varphi', \qquad -1 < \varphi < 1. \tag{5.2}$$

We also wrote the pressure jump condition on the bubble surface in the form

$$b^2(x_\varphi^2 + y_\varphi^2)^{-1} = (y_{\varphi\varphi}x_{\varphi\varphi} - x_{\varphi\varphi}y_{\varphi\varphi})(x_\varphi^2 + y_\varphi^2)^{-3/2} - \gamma, \qquad -1 < \varphi < 1, \quad \psi = 0. \tag{5.3}$$

In addition, the symmetry about the x-axis yielded

$$\lim_{\varphi \to \pm 1} \frac{y_\varphi(\varphi, 0)}{x_\varphi(\varphi, 0)} = \infty. \tag{5.4}$$

These equations (5.2)–(5.4) constituted the problem for the determination of $x_\varphi(\varphi, 0)$, $y_\varphi(\varphi, 0)$ and b for a given value of the parameter γ.

To solve these equations, we required the bubble to be symmetric about the y-axis and therefore about the φ-axis. Then we could restrict our considerations to the interval $0 \leqq \varphi < 1$ with $y_\varphi(0, 0) = 0$. Within this interval we introduced the new variable α in place of φ by the equation $\varphi = 1 - \alpha^2$. This eliminated from the solution the singularities at the stagnation point $\varphi = 1$, $\psi = 0$. Once this new variable was defined, we introduced mesh points and values of the unknown functions at the mesh points just as in the previous section. By proceeding in the manner described there, we converted the equations above into a set of nonlinear algebraic equations for b and the values of y_φ at the mesh points.

To solve these equations by Newton's method for a given value of γ, we needed an initial approximation to the solution. Therefore we determined the asymptotic form of the solution for γ large, when the bubble tends to a circle of radius γ^{-1}. We used this as the initial approximation for a large value of γ and iterated until we obtained a solution. Then we used that solution as the initial approximation for a slightly smaller value of γ, and so on.

Three of the resulting bubbles are shown in Fig. 6 for $\gamma = 2.3$, 0.0, and 0.42. At $\gamma = 0.42$ the opposite sides of the bubble just touched one another on the x-axis. The bubble might then split into two bubbles. For $\gamma = 0$ our result agreed with the analytic solution obtained by E. B. McLeod [12] in this special case.

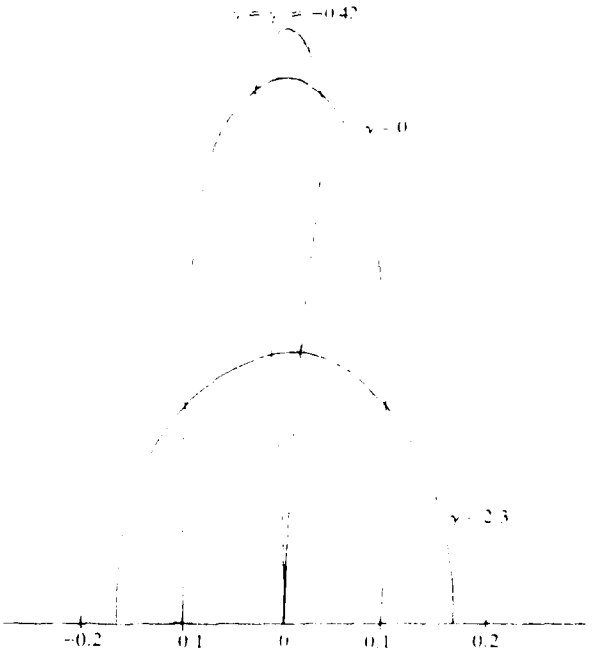

FIG. 6. *One half of the computed bubble profiles for* $\gamma = 2.3$, $\gamma = 0$ *and* $\gamma = \gamma_{cr} = -0.42$.

The half-bubbles shown in Fig. 6 also represent bubbles attached to a wall with contact angle $\beta = \pi/2$. We also determined the shapes of bubbles attached to a wall with other values of β by a suitable modification of the preceding method. The difference in the formulation was that the right side of (5.4) was replaced by $\pm\tan\beta$. Then in changing variables we set $\varphi = 1 - \alpha^{\pm\beta}$.

For each value of β, the bubble began as a circular arc of radius γ^{-1} for γ very large, and it deformed as γ was decreased. Finally a value of γ, which we called $\gamma_{cr}(\beta)$, was reached at which opposite sides of the bubble came into contact with one another. For $\beta \leqq \pi/2$ the contact occurred on the wall as in Fig. 6. However for $\beta > \pi/2$, it occurred off the wall as is shown in Fig. 7 for $\beta = 2\pi/3 = 120^\circ$. Bubbles are presented in that figure for $\gamma = 1.3$, $\gamma = -0.6$ and $\gamma = \gamma_{cr}(2\pi/3) = -1.6$. The negative values of γ indicate that the pressure in the bubble is less than the stagnation pressure. If the bubble breaks into two at the point of contact, part of the bubble will be off the wall and part will remain attached to the wall, and our calculation determines the size of each.

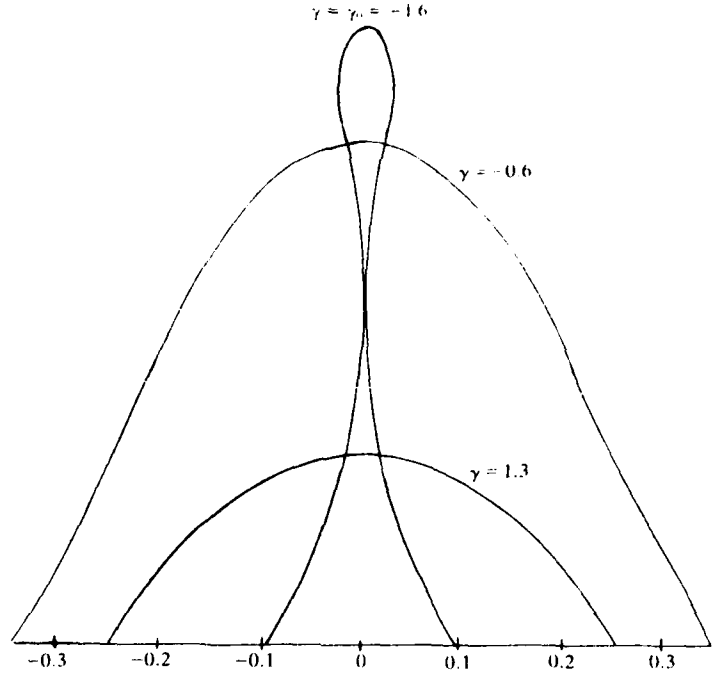

FIG. 7. *Three computed profiles for a bubble on a wall with contact angle* $\beta = 120°$ *and* $\gamma = 1.3$, $\gamma = -0.6$ *and* $\gamma = \gamma_0 = -1.6$. *At* $\gamma = \gamma_0 = -1.6$, *the bubble touches itself at about the distance* $y = 0.35$ *from the wall.*

6. Bubble distortion in a straining flow. In the mixing of two fluids, a drop of one fluid may be broken up into smaller drops by the action of the other fluid flowing around it. To investigate this process J.-M. Vanden-Broeck and I [13] considered the distortion of a drop or bubble in a straining flow, a problem proposed to us by Professor A. Acrivos. As in the preceding section, we treated the two-dimensional case of a constant pressure bubble or drop in an inviscid, incompressible fluid. The stream function of the flow was assumed to be αxy far from the bubble.

The formulation of this problem and the method of solution were very similar to those of the preceding section, so we shall just indicate the differences and then describe the results. The length scale we chose was $(2\sigma/\rho\alpha^2)^{1/3}$, the velocity scale was $(2\sigma\alpha/\rho)^{1/3}$, and then the sole dimensionless parameter was γ defined by

$$\gamma = 2(p_s - p_b)/(2\sigma\alpha)^{2/3}\rho^{1/3}. \tag{6.1}$$

Because of the symmetry of the incident flow, it sufficed to solve the problem in the angular sector $0 \leqq \theta \leqq \pi/4$ with $\theta = 0$ a streamline and $\theta = \pi/4$ a potential line. We then introduced new variables, used the Hilbert transform, introduced a mesh and difference formulas, etc. Finally we solved the resulting equations by Newton's method.

The calculated bubbles for three values of γ are shown in Fig. 8. As $\gamma \to \infty$, the bubble tends to a circle of radius γ^{-1}, and the bubble shown for $\gamma = 5$ is still close to a circle. However when γ has decreased to zero, the bubble is nearly a square with rounded corners. This is understandable because there are four stagnation points where the bubble meets the x and y axes. At them, the fluid pressure is maximal and it pushes the bubble surface inward. When $\gamma = -1.24$ these four points have moved further in

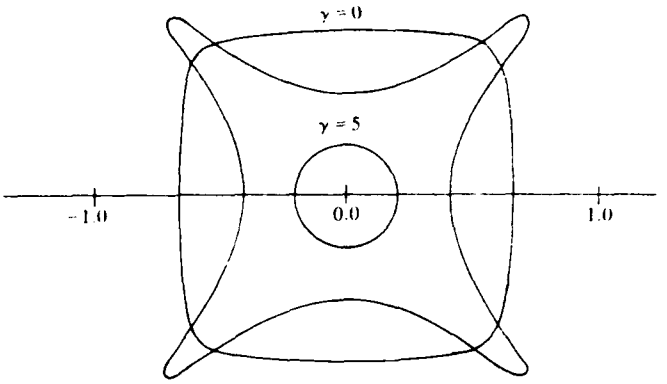

FIG. 8. *Computed profiles of a bubble in a straining flow with* $\gamma = 5$, $\gamma = 0$ *and* $\gamma = -1.24$.

while in between adjacent pairs of them four horns or spikes have appeared. We have also determined the ultimate form of the horns as γ is further decreased. We find that near each tip opposite sides come into contact with one another and form a small bubble there.

7. Damping of underwater explosion bubble oscillations. Now we shall consider a time dependent problem, the oscillation of the gas bubble produced by the detonation of an explosive charge under water. Such a bubble is initially small, spherical, and at very high pressure. It expands rapidly, remaining spherical and pushing the water radially outward. When the bubble pressure reaches the ambient value, the water is still moving outward, causing the bubble to overexpand. When the expansion finally stops, the bubble begins to contract but the inertia of the water again causes it to overcontract and the process repeats itself. In this way the radial oscillations of underwater explosion bubbles are produced. The dots in Fig. 9 are experimental values of the radius of one such bubble at different times after detonation, and they show the typical oscillations.

In 1916, Rayleigh formulated the theory of these oscillations on the assumption that the water was inviscid and incompressible. His theory yielded undamped periodic oscillations because it did not contain any mechanism for energy loss. It was later realized that acoustic radiation was the main loss mechanism. This was verified by

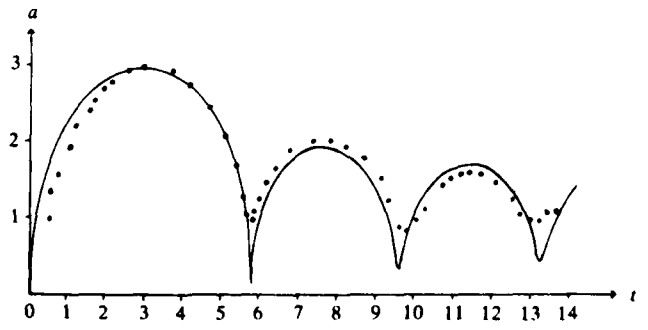

FIG. 9. *The bubble radius as a function of time for a 0.55 lb. charge of tetryl detonated at a depth of 300 ft. below the water surface. The dots are experimental points and the solid curve is calculated from (7.4). The unit of length is* $\bar{a} = 6$ *inches and the unit of time is* $\bar{a}(\rho p_0^{-1})^{1/2} = 4.85$ *milliseconds.*

estimating the acoustic loss, calculating the consequent damping, and comparing the result with observations.

To incorporate the loss mechanism into the theory, I. I. Kolodner and I [14], in 1951, developed a new theory of the oscillation taking account of the compressibility of the water. We did so by using the wave equation for the potential function of the water motion, rather than Laplace's equation which Rayleigh had used.

The use of the wave equation to describe large amplitude motions was considered inappropriate at that time, and it still is so considered by many fluid dynamicists. On the other hand, the less accurate Laplace equation is regarded as perfectly suited to describe such motions. This difference in attitude is probably due to the differences in the methods of derivation of the two equations. In the derivation of the wave equation, the smallness of the velocity is emphasized to justify linearization of the compressibility terms. However in the derivation of Laplace's equation, the compressibility terms are just ignored from the beginning, so it is never necessary to mention that the velocity is small.

Our theory of the bubble oscillation is based on the assumption that the pressure $P(a)$ in the bubble is a function of the bubble radius $a(t)$, given by the adiabatic relation

$$P(a) = k[4a^3/3]^{-\gamma}. \tag{7.1}$$

Here k and γ are given constants. The potential function $\varphi(r, t)$ of the water motion is assumed to satisfy the wave equation with sound speed c:

$$\Delta\varphi - c^{-2}\varphi_{tt} = 0. \tag{7.2}$$

Then the pressure $p(r, t)$ in the water is given by the Bernoulli equation

$$p(r, t) = p_0 - \rho(\varphi_t + \tfrac{1}{2}\varphi_r^2), \tag{7.3}$$

where p_0 is the initial pressure and ρ is the density of the water. The formulation is completed by requiring the pressure $p(a, t)$ in the fluid to equal that in the bubble, $P(a)$, at $r = a$, and requiring the fluid velocity $\varphi_r(a, t)$ to equal a_t at $r = a$. We also give the initial radius and velocity of the bubble and assume that $\varphi = \varphi_t = 0$ for $r > a$ at $t = 0$.

From this formulation we derived the following autonomous nonlinear second-order ordinary differential equation for $a(t)$:

$$(a_t - c)(aa_{tt} + \tfrac{3}{2}a_t^2 - \Delta) - a_t^3 + a^{-1}(a^2\Delta)_t = 0. \tag{7.4}$$

Here $\Delta(a)$ is defined by

$$\Delta(a) = \rho^{-1}[P(a) - p_0]. \tag{7.5}$$

If we divide (7.4) by c and let c become infinite, we obtain Rayleigh's equation for $a(t)$. A phase plane analysis shows that the equilibrium point of (7.4) is a spiral point, corresponding to damped oscillations, while that of Rayleigh's equation is a center, representing periodic oscillations.

In Fig. 9 the solid curve represents the solution of (7.4) obtained numerically for initial conditions corresponding to the bubble whose observed radius is given by the dots. We see that the theoretical curve is in good agreement with the observed data, and it correctly predicts the damping of the radial motion due to the radiation of acoustic energy. From $a(t)$ the pressure pulses radiated by the bubble can be found.

8. Forced oscillations of a gas bubble in a sound field. To describe the oscillation of small bubbles in a fluid, such as cavitation bubbles or air bubbles, it is necessary to take into account surface tension and viscosity as well as inertia. Therefore, Plesset [15] and others modified Rayleigh's equation to include these effects. They also included an external time dependent pressure, representing an incident sound field.

Lauterborn [16] solved the modified equation numerically for periodic incident sound fields, seeking periodic oscillations of the bubble. He obtained them for small and moderate values of the amplitude of the applied pressure. From his results he plotted a response curve for each applied pressure, showing the maximum bubble radius of the periodic solution as a function of the applied frequency. However, for very large amplitudes of the applied pressure, the solution did not become periodic; or if it did, the amplitudes did not lie on a smooth curve.

It seemed to me that this difficulty with the large amplitude oscillations could be avoided by taking into account the acoustic radiation from the bubble, just as was done in the preceding section to describe the damping of underwater explosion bubble oscillations. Therefore my student M. Miksis and I [17] modified (7.4), the equation of Keller and Kolodner, to include surface tension, viscosity and an incident sound field, in the same way as Plesset and others had modified Rayleigh's equation.

The equation we derived in this way is

$$a a_{tt}\left[\frac{4\mu}{\rho} - a(a_t - c)\right] = \frac{1}{2}a_t^3 + a_t\Delta(a) - c\left[\frac{3}{2}a_t^2 + \frac{4\mu a_t}{\rho a} - \frac{2\sigma}{\rho a} - \Delta(a)\right] + aa_t\Delta'(a) + 2\left(1 + \frac{a_t}{c}\right)g''(t + a/c). \tag{8.1}$$

Here $a(t)$ is the bubble radius at time t, c is the sound speed in the fluid, ρ is the fluid density, μ is the coefficient of viscosity of the fluid, σ is the surface tension, $2c^{-1}g''$ is the time derivative of the potential of the incident sound field evaluated at the center of the bubble and $\rho\Delta(a)$ is the difference between the bubble pressure and the pressure at infinity. The pressure in the bubble was taken to be $ka^{-3\gamma} + p_v$, where p_v represents a constant vapor pressure and k and γ are constants. When $c = \infty$, (8.1) reduces to the equation solved by Lauterborn; while when $\mu = v = g = p_v = 0$, it reduces to the equation (7.4) of Keller and Kolodner.

To treat this equation we first studied the free oscillations corresponding to $g = 0$ by a phase plane analysis, and obtained results like those of Keller and Kolodner [14]. We also solved (8.1) numerically for the same case shown in Fig. 9 and obtained the same result because surface tension and viscosity are negligible in that case.

Next we chose $2c^{-1}g''(t) = \rho^{-1}P \sin \omega t$, which is the same forcing function as was used by Lauterborn [16]. Then we solved the equation analytically by the method of averaging, in the same way as Prosperetti [18] had solved the equation used by Lauterborn. The results were similar to his, showing harmonic, subharmonic and ultraharmonic resonances.

Finally we solved the equation numerically as an initial value problem, as Lauterborn did. Some of our results are shown in Fig. 10. They agree with his except at the largest forcing amplitudes. Then our equation yields periodic solutions and a response curve similar to those which we both found for smaller amplitudes, whereas his did not. Thus the inclusion of the effects of acoustic radiation in (8.1) has had the desired effect of yielding periodic oscillations and a response curve for even very large amplitudes of the incident pressure field.

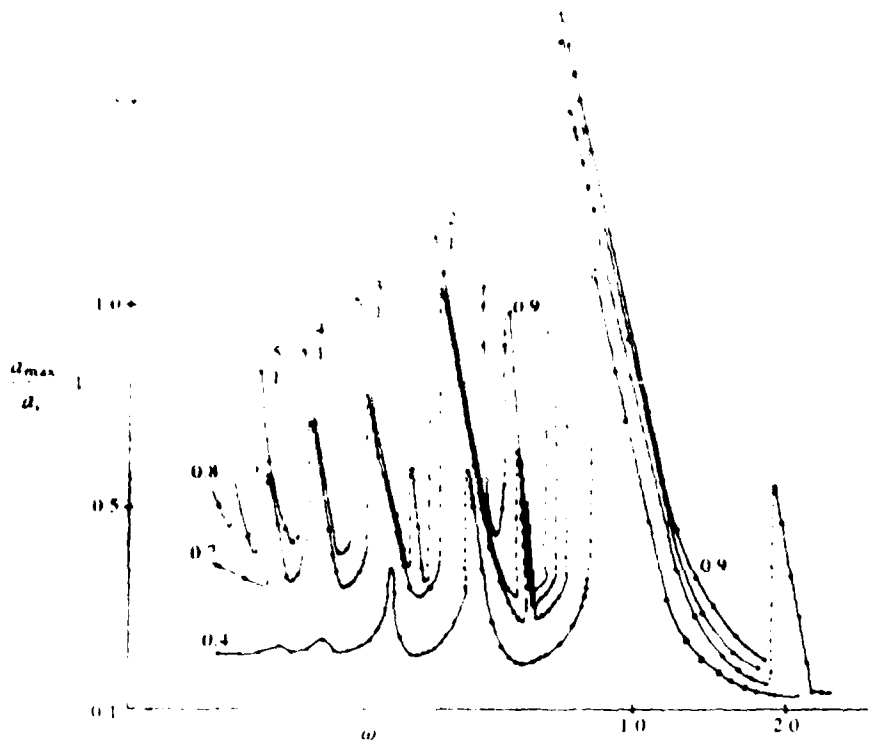

FIG. [illegible] Computed response curves for a bubble in a periodic sound field. The vertical axis shows the maximum radius of the bubble minus its equilibrium radius all divided by the equilibrium radius, $(a_{max} - a_e)/a_e$. The horizontal axis is the ratio of the incident sound wave frequency to the free vibration frequency of the bubble. The four response curves are for amplitudes of the incident sound field equal to 0.4, 0.7, 0.8 and 0.9 bar, respectively. The other parameters correspond to a bubble of radius $a_e = 10\ \mu m$ in water with a static pressure of 1 bar.

REFERENCES

[1] G. B. WHITHAM, *Linear and Nonlinear Waves*, Wiley, New York, 1974.

[2] J. F. FLAHERTY, J. B. KELLER AND S. I. RUBINOW, *Post buckling behavior of elastic tubes and rings with opposite sides in contact*, SIAM J. Appl. Math., 23 (1972), pp. 446–455.

[3] I. TADJBAKHSH AND F. ODEH, *Equilibrium states of elastic rings*, J. Math. Anal. Appl., 18 (1967), pp. 59–74.

[4] H. ZELLER AND R. WIRTZ, *Buckling behaviour of rubber and PVC tubes*, Aerodynamisches Institut, Technische Hochschule, Aachen, Germany, preprint.

[5] C. BROOKS AND A. B. LUCKHARDT, *The chief physical mechanisms concerned in clinical methods of measuring blood pressure*, Amer. J. Physiology, 40 (1916), pp. 49–74.

[6] J. P. HOLT, *Flow of fluids through collapsible tubes*, Circulation Research, 7 (1959), pp. 342–353.

[7] ———, *The collapse factor and measurement of venous pressure. The flow of fluid through collapsible tubes*, Amer. J. Physiology, 134 (1941), pp. 292–299.

[8] J. E. FLAHERTY AND J. B. KELLER, *Contact problems involving a buckled elastica*, SIAM J. Appl. Math., 24 (1973), pp. 215–225.

[9] J. D. CRAPPER, *An exact solution for progressive capillary waves of arbitrary amplitude*, J. Fluid Mech., 2 (1957), pp. 532–540.

[10] J.-M. VANDEN BROECK AND J. B. KELLER, *A new family of capillary waves*, Ibid., 98 (1980), pp. 161–169.

[11] ———, *Deformation of a bubble or drop in a uniform flow*, Ibid., in press.
[12] F. B. MCLEOD, *The explicit solution of a free boundary problem involving surface tension*, J. Rational Mech. Anal., 4 (1955), pp. 557–567.
[13] J.-M. VANDEN-BROECK AND J. B. KELLER, *Bubble or drop creation in a straining flow in two dimensions*, Phys. Fluids, in press.
[14] J. B. KELLER AND I. I. KOLODNER, *Damping of underwater explosion bubble oscillations*, J. Appl. Phys., 27 (1956), pp. 1152–1161.
[15] M. S. PLESSET, *The dynamics of cavitation bubbles*, J. Appl. Mech., 16 (1949), pp. 277–282.
[16] W. LAUTERBORN, *Numerical investigation of nonlinear oscillations of gas bubbles in liquids*, J. Acoust. Soc. Amer., 59 (1976), pp. 283–293.
[17] J. B. KELLER AND M. MIKSIS, *Bubble oscillations of large amplitude*, Ibid., in press.
[18] A. PROSPERETTI, *Thermal effects and damping mechanisms in the forced radial oscillations of gas bubbles in liquids*, Ibid., 61 (1977), pp. 17–27.

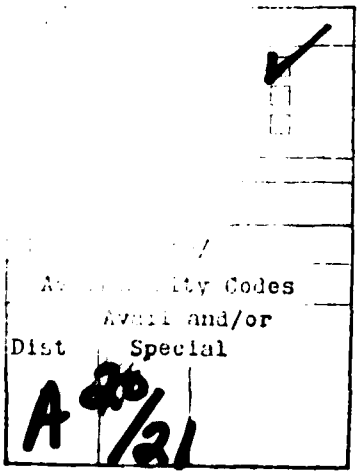

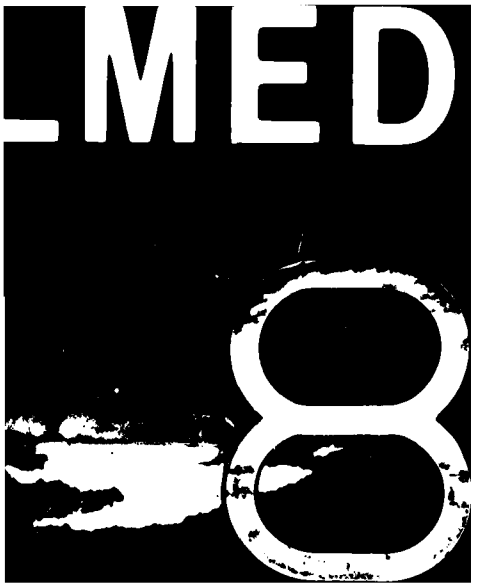
LMED
8